The saturation of the fluorescence and its consequences for laser-induced fluorescence thermometry in liquid flows

William Chaze, Ophélie Caballina, Guillaume Castanet, Fabrice Lemoine

The saturation of the fluorescence and its consequences for laser-induced fluorescence thermometry in liquid flows

William Chaze[1,2] · Ophélie Caballina[1,2] · Guillaume Castanet[1,2] · Fabrice Lemoine[1,2]

Abstract The temperature dependence of the fluorescence emission of certain organic dyes such as rhodamine B has been widely utilized for measuring the temperature in liquid flows. Measurements are generally based on two assumptions: The fluorescence signal is proportional to the intensity of the laser excitation, and the temperature sensitivity of the dye is not affected by the laser irradiance. In the ratiometric methods, these assumptions allow justifying that the influence of the laser intensity can be totally eliminated in the intensity ratio of two spectral bands of the fluorescence emission and thus that measurements can be taken with no biases under experimental conditions, where the laser propagation is disturbed by the flow. However, when pulsed lasers are used (mainly in planar LIF measurements), the peak irradiance usually compares or exceeds the saturation intensity of the dyes. The present study assesses the consequences of a saturation of the dye emission on temperature measurements. Tests among fluoresceins and rhodamines reveal that the saturation can be accompanied by a significant loss of temperature sensitivity. The dyes, for which this loss of sensitivity is observed, mainly owe their temperature dependence to the fluorescence quantum yield and have a fluorescence signal decreasing with the temperature. The couple fluorescein/sulforhodamine 640 is finally proposed for an implementation of the ratiometric method, since its relatively high temperature dependence (+3 %/°C) is not altered at high laser irradiances. The possibility of measuring instantaneous temperature fields with this pair of dyes using a single laser shot is finally demonstrated on a turbulent heated jet injected into quiescent water.

✉ Guillaume Castanet
guillaume.castanet@univ-lorraine.fr

[1] LEMTA, UMR 7563, Université de Lorraine, 54500 Vandœuvre-Lès-Nancy, France

[2] LEMTA, UMR 7563, CNRS, 54500 Vandœuvre-Lès-Nancy, France

1 Introduction

Soluble dyes for aqueous flows have long been used to visualize flows in fluid mechanics. When quantitative measurements are required, the choice is usually made to use fluorescent dyes and measure the concentration in fluorescent molecules using approaches based on laser-induced fluorescence (LIF). Scalar concentrations can be measured at a point, along the line of a laser beam, but the most common application of LIF in fluid flows is two-dimensional planar laser-induced fluorescence (PLIF). In the presence of heat transfers, nonintrusive measurements of the temperature are also very useful and interesting. Such measurements are made possible by some organic dyes which have a temperature-dependent fluorescent emission. The dyes selected for the purpose of temperature measurements have specific properties. In particular, their fluorescence quantum yield and/or their absorption cross section at the excitation wavelength should be highly dependent on temperature. Ideally, they also exhibit a certain degree of resistance to photodegradation. As an example, rhodamine B and Kiton red have widespread applications in water solutions to determine the temperature in flows induced by natural convection (Coolen et al. 1999; Sakakibara and Adrian 2004) or to study turbulent mixing in plumes or jets (Sakakibara and Adrian 1999; Bruchhausen et al. 2005; Lemoine et al. 1999).

Methods for measuring the temperature in liquid flows have evolved over time, and several approaches, more

or less easy to implement, are now available. Techniques using a single dye and a single spectral band for the detection of the LIF signal have historically been the first developed (Nakajima et al. 1990; Lemoine et al. 1999; Sakakibara et al. 1993; Coolen et al. 1999). The temperature is directly deduced from the variations in the fluorescence intensity relative to a reference measured at a known temperature. Hence, any disturbance of the LIF signal that does not pertain from the temperature leads to a measurement error. Extreme care is thus required to maintain the concentration of dye molecules and the laser light constant during the experiments. If a pulsed laser is used, the pulse energy has to be monitored in order to account for the shot-to-shot fluctuations in energy of the laser. Nevertheless, in practice, variations in refractive index that may arise from temperature gradients in the flow (shadowgraph effect) generally prevent the distribution of laser light from remaining the same in successive measurements (Coolen et al. 1999). Changes in refractive index also disturb the propagation of fluorescent light on its way to the detector. As a result, observed variations in fluorescence signal do not exclusively originate from temperature changes in the excitation volume. In multiphase flows, the mobile and curved interfaces of droplets and bubbles can also modify light propagation. Thus, the single-band/single-dye (1c/1d) approach usually fails to measure the temperature in sprays and bubbly flows.

Most of the above problems can be avoided or limited with ratiometric techniques. This explains why these techniques have become almost unavoidable despite more equipment is generally required for their implementation. The fluorescence signal emitted on two spectral bands is detected separately, and the temperature is deduced from the ratio between the intensities of these two bands, also called in the following the fluorescence ratio. In several studies, a temperature-sensitive dye is associated with a reference dye almost insensitive to the temperature (Sakakibara and Adrian 1999, 2004). In other studies, the associated dyes have opposite responses to the temperature, which allows obtaining relatively high sensitivities of the ratio to the temperature (Sutton et al. 2008). One difficulty of these methods, referred hereafter as two-color/two-dye (2c/2d) techniques, is to find two dyes with a limited overlap between their emission and absorption spectra to avoid spectral conflicts (Coppeta and Rogers 1998). Alternatively, ratiometric techniques can exploit the deformation of the fluorescence spectrum with the temperature. In these approaches, only one dye is used and two spectral bands with very different sensitivities to the temperature are detected simultaneously. The two-color/one-dye (2c/1d) method has been implemented in single-phase flows (Bruchhausen et al. 2005), in droplet streams and sprays (Lemoine and Castanet 2013; Castanet et al. 2011; Labergue et al. 2013). This approach is recommended when the dye concentration is not uniform, for example in the presence of mass transfers such as liquid evaporation/vapor condensation. In contrast, the ratio of the concentrations of the two dyes must be kept constant in the 2c/2d techniques.

Whether one or two fluorescent dyes are used for the measurements, ratiometric techniques allow eliminating the dependence on laser irradiance provided that the LIF signal is proportional to the laser intensity. This proportionality is not a problem when continuous-wave lasers like ionized gas lasers are utilized as it was the case of many early studies where the 2c/2d and 2c/1d approaches were implemented (Sakakibara and Adrian 1999, 2004; Hishida and Sakakibara 2000; Kim and Yoda 2010; Shafii et al. 2010; Dunand et al. 2012). The laser irradiance in these applications where 2D temperature fields were characterized is relatively low (typically on the order of a few hundreds of W/cm^2). Today, pulsed lasers are more and more utilized for PLIF imaging. In particular, pulsed Nd:YAG lasers deliver tens or hundreds of mJ in a few ns, which can easily result in peak intensities of a few tenth of MW/cm^2 in the laser sheet for most applications. These levels of laser irradiance are significantly higher than the saturation intensity I_{sat} of most fluorescent dyes (Crimaldi 2008). Values of I_{sat} have been estimated or inferred for rhodamine 6G (Shan et al. 2004) and rhodamine WT (Melton and Lipp 2003) to be of order 1 MW/cm^2. When pulsed lasers are used to induce the fluorescence, it is thus common to have partially saturated fluorescence. This latter remark gives rise to questions about the relevance of ratiometric methods with pulsed lasers. Furthermore, as the fluorescence signal is not the function of the quantum yield in the saturated regime, fluorescent dyes like rhodamine B are expected to lose totally or partially their sensitivity to temperature at high flux excitation. This effect was seldom reported in early studies but may be of importance for applications of LIF thermometry using pulsed lasers. At the same time, the high radiation power of pulsed laser is a great advantage for planar measurements. As cameras receive considerable signal in a very short period of time, it becomes possible to perform instantaneous measurements of temperature fields, meaning that a single laser shot is sufficient to obtain the temperature with a reasonable accuracy (typically on the order of 1 °C). In the applications of two-color PLIF using pulsed Nd:YAG lasers reported so far, temperature measurements generally proceed of an averaging that can be an integration of the signal over several laser shots or the summation of several images (Bruchhausen et al. 2005; Vetrano et al. 2013; Düwel et al. 2004), as the accumulation of laser shots and images allows improving the signal-to-noise ratio. When the laser irradiance is increased, the need for cumulative laser shots could be reduced until only one laser

shot becomes sufficient for quantitative measurements, provided that the saturation of the fluorescence is not reached before with a detrimental effect on the temperature sensitivity of the measurements.

In the present study, ratiometric methods, both the 2c/1d and the 2c/2d approaches, are evaluated in the regime of a partially saturated fluorescence. Potential errors arising from the nonlinearity of the fluorescence signal and the loss of temperature sensitivity at high-power excitation are highlighted and quantified for several examples of dyes and associations of spectral bands. Also, an interesting pair of dyes (fluorescein disodium/sulforhodamine 640) for 2c/2d measurements is proposed for the measurements with pulsed Nd:YAG lasers at 532 nm as its temperature sensitivity is high and almost insensitive to the laser irradiance. The possibility of instantaneous one-shot temperature measurements with this pair of dyes is finally demonstrated in an example of application consisting in the observation of the thermal mixing in a turbulent water jet.

2 Fluorescence signal at high-power excitation

Fluorescence is a form of luminescence which results from the spontaneous emission of a photon by a molecule which has been excited to a quantum state of higher energy corresponding to a singlet state. When the excited molecule returns to its ground state, many pathways can compete with spontaneous emission including collisional quenching, intersystem crossing, internal conversion, quenching by energy transfer, and charge transfer reaction. All these mechanisms contribute to a quenching of the fluorescence emitted by the population of molecules. At high-power laser excitation, stimulated emission can also occur (Fig. 1).

Two energy levels, one corresponding to the ground state 1 and the other to the excited state 2, are generally considered to describe the fluorescence process (Lee 2008). In the following, N_1 and N_2 denote the number densities of the molecules in the energy states 1 and 2, respectively. The time rates of change for the populations N_1 and N_2, due to either upward or downward transitions, can be expressed as:

$$\frac{\mathrm{d}N_2}{\mathrm{d}t} = -\frac{\mathrm{d}N_1}{\mathrm{d}t} = N_1\, b_{12} - N_2(b_{21} + A_{21} + Q_{21}), \tag{1}$$

where b_{12} is the rate constant for the transition from 1 to 2 due to photon energy absorption. The parameters b_{21}, A_{21}, and Q_{21} are, respectively, the rate constant for the transition from 2 to 1 due to stimulated photon emission, spontaneous photon emission, and quenching. Because absorption and stimulated emission are induced by resonant photons, their rate constants depend on the spectral radiance of the incident laser light I_λ at the frequency of the transition:

$$b_{12\text{ or }21} = \frac{B_{12\text{ or }21}\, I_\lambda}{C_\lambda}, \tag{2}$$

where $B_{12} = B_{21}$ are the Einstein's coefficients for absorption and stimulated emission, and C_λ is a conversion faction having the same unit as I_λ. Initially, the molecules are at the ground state, so $N_1 = N_1^0$ and $N_2 = 0$ at $t = 0$. Since at all times $N_1 + N_2 = N_1^0$, Eq. (1) can be rewritten:

$$\frac{\mathrm{d}N_2}{\mathrm{d}t} = b_{12}\, N_1^0 - N_2 \frac{1}{\tau}, \tag{3}$$

where $\tau = (b_{12} + b_{21} + A_{21} + Q_{21})^{-1}$ is the fluorescence lifetime. Assuming the duration of the laser illumination is sufficiently long in comparison with the lifetime τ, the system reaches a steady state given by:

$$N_2 = \frac{B_{12}}{A_{21} + Q_{21}} \frac{I_\lambda}{\left(1 + \frac{I_\lambda}{I_{\mathrm{sat}}}\right)} N_1^0, \tag{4}$$

where $I_{\mathrm{sat}} = \frac{A_{21}+Q_{21}}{B_{12}+B_{21}} C_\lambda$ is the saturation irradiance. The fluorescence signal intensity using the steady-state solution (4) can be expressed as:

$$F_\lambda \propto A_{21} N_2 = B_{12}\, \phi_\lambda \frac{I_\lambda}{\left(1 + \frac{I_\lambda}{I_{\mathrm{sat}}}\right)} N_1^0, \tag{5}$$

where $\phi_\lambda = A_{21}/(A_{21} + Q_{21})$ is the fluorescence quantum yield (QY). In Eq. (5), N_1^0 is the initial number density of the molecules in a particular energy state on which the incident laser is tuned to induce an upward transition. In fact, there are many possible energy states for the molecules (corresponding to rotational and vibrational degrees of freedom) and the temperature will affect the distribution of energy states among the molecules The fraction of molecules in the energy state corresponding to the considered transition is given by the Boltzmann fraction $f_B(T)$. Based on Eq. (5), the fluorescence signal detected by a photodetector from a collection volume V can be expressed as:

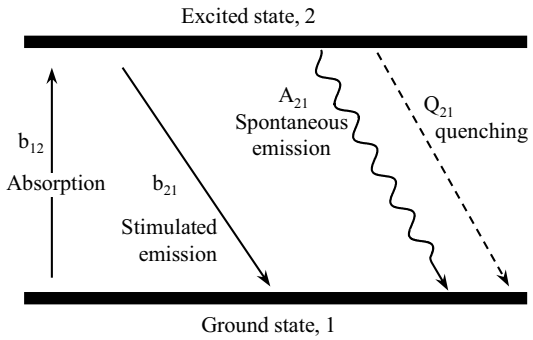

Fig. 1 A two-level diagram of laser-induced fluorescence

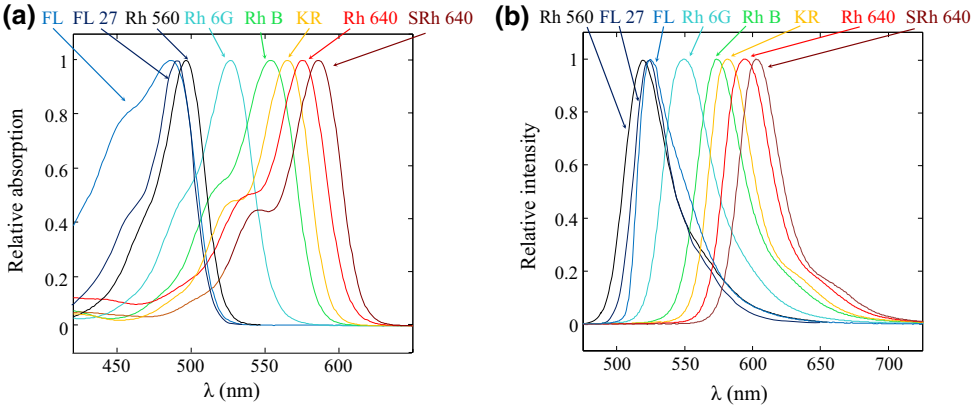

Fig. 2 Absorption and emission spectra measured at 25 °C (pH 5.6 for FL and pH 6.5 for RhB)

$$F_\lambda = \eta \frac{\Omega}{4\pi} \varepsilon \, \phi_\lambda \frac{I_0}{\left(1 + \frac{I_0}{I_{\text{sat}}}\right)} V \, C, \tag{6}$$

where η is the transmission efficiency of the collection optics, Ω is the solid angle of collection, C is the molar concentration of the dye molecules in the liquid medium, ϕ_λ is the fluorescence QY, and I_0 (W.m^{-2}) corresponds to the intensity of the incident laser beam. The factor $\varepsilon \propto B_{12} \cdot f_B(T)$ denotes the molar extinction coefficient of the fluorescent molecules at the excitation wavelength. Using Eq. (6) and remembering that $I_{\text{sat}} \propto 1/\phi_\lambda$, the temperature dependence of the fluorescence signal can be determined:

$$\frac{F_\lambda(T)}{F_\lambda(T_0)} = g_{0,\lambda}(T) \cdot \frac{1 + \frac{I_0}{I_{\text{sat}}(T_0)}}{1 + g_{0,\lambda}(T) \cdot \frac{I_0}{I_{\text{sat}}(T_0)}} \cdot \frac{\varepsilon(T)}{\varepsilon(T_0)}. \tag{7}$$

In this expression, T_0 is an arbitrary temperature of reference and $g_{0,\lambda}(T) = \phi_\lambda(T)/\phi_\lambda(T_0)$. Based on Eq. (7), the temperature sensitivity of the fluorescence signal originates from two contributions. One is the variation in the QY with the temperature, and the second corresponds to the temperature dependence of the absorption cross section at the laser wavelength. Equation (7) demonstrates that the quenching contribution vanishes when the irradiance of the laser exceeds the saturation threshold $I_{\text{sat}}(T_0)$. The consequences for temperature measurement is discussed hereafter in the case of several dyes including several rhodamines and fluoresceins.

3 Temperature dependence of fluorescent dyes

The organic dyes tested in the present study include rhodamine B (RhB), kiton red (KR), rhodamine 560 (Rh560), rhodamine 640 (Rh640), rhodamine 6G (Rh6G), sulforhodamine 640 (SRh640), fluorescein disodium (FL), and fluorescein 27 (FL27). These dyes have in a common that they can absorb the radiation at 532 nm of the Nd:YAG lasers used in the experiments and emit fluorescence in return (Fig. 2). Also, for most of them, an application to temperature measurement in water solutions has already been reported (Bruchhausen et al. 2005; Coppeta and Rogers 1998; Dunand et al. 2012; Natrajan and Christensen 2009; Sakakibara and Adrian 1999; Sutton et al. 2008).

3.1 Temperature dependence in the regime of weak excitation

A CW frequency-doubled Nd:YAG laser (532 nm) was used for the excitation of the dyes. The moderate output power of the CW lasers (on the order of a few W) guarantees that the irradiance of the laser beam is far below the saturation threshold I_{sat} in the conditions of the experiments. Typically, the laser irradiance is about 1 W/cm^2 in the experiments which are reported in this section. Emission and absorption spectra measured at 25 °C are displayed in Fig. 2. Spectra are shifted from one dye to another which is very important for selecting pairs of dyes with limited spectral conflicts in the 2c/2d method as explained later in Sect. 5. A known issue for measuring emission spectra relates to the absorption of the fluorescence by the dye itself before that fluorescence has reached the detector positioned at right angle relatively to the laser beam. To limit this effect, the dye concentration was set to a very low value (on the order of 10^{-6} mol/L) with the noticeable exceptions of FL and FL27. For these dyes, a much higher concentration of 10^{-4} mol/L was required due to their small absorption cross section at 532 nm. The consequence is a significant reabsorption below 520 nm even if optical paths are limited to a few mm in the experiments.

In practice, some precautions are needed to limit the photodegradation of the dyes. A measurement cell with a relatively large volume (typically 1 L or more) is utilized in the experiments. The liquid is stirred, which allows a fast renewal of the dye molecules excited by the laser beam. The laser is switched on only during the signal acquisition,

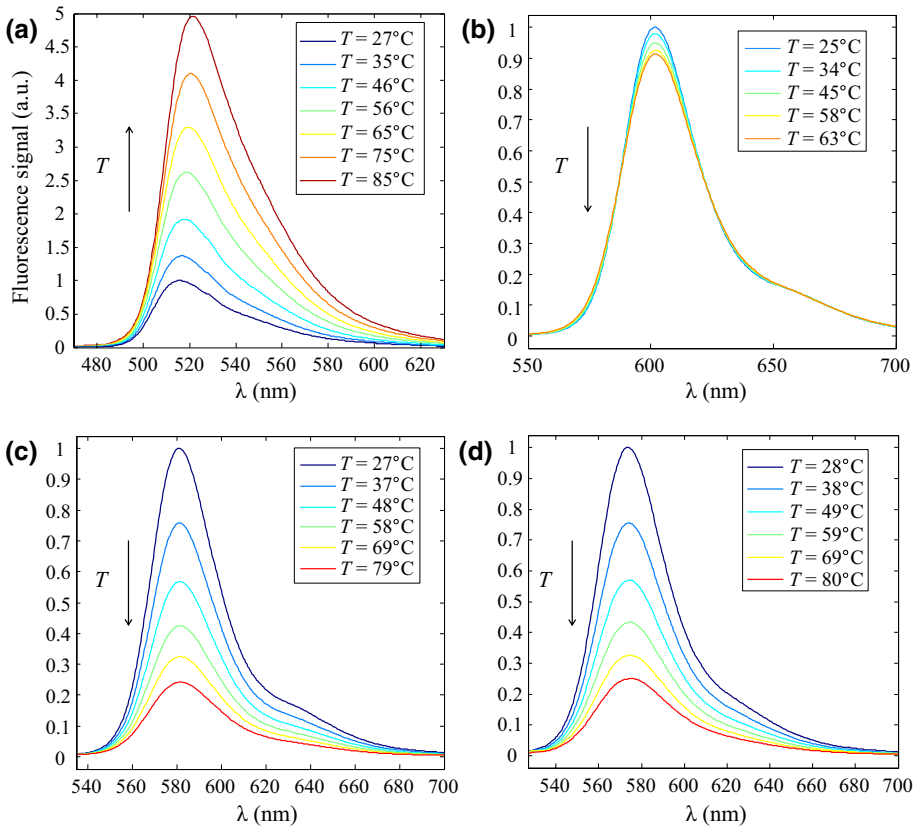

Fig. 3 Emission spectra of some fluorescent dyes measured at different temperatures (**a** FL at pH 5.6, **b** SRh640, **c** KR, and **d** RhB)

which avoids any photodamage the rest of the time. The precautions described above were applied in all the measurements reported in Sect. 3 including the ones performed with a pulsed laser.

The emission spectra of the dyes were recorded for temperatures ranging from 25 to 85 °C. Results are shown in Fig. 3 in the case of FL, KR, RhB, and SRh640. Very different behaviors of the dyes can be observed in this figure. In the case of FL at pH 5.6, the fluorescence signal strongly increases with the temperature, while a sharp decrease can be pointed out for KR and RhB. Also, the temperature dependence is very limited in the case SRh640. Variations can be pointed out essentially near the peak of the emission spectrum of SRh640 (Fig. 3b). It should also be noted that the molecules of Rh640 and SRh640 can be damaged by thermal heating. These reactions proceed at a relatively fast rate above 60 °C (about 5 % of the molecules of SRh640 disappear after one hour at 60 °C and 15 % at 80 °C). This explains why the range of temperature change is more limited for SRh640 in Fig. 3.

The emission spectra measured at different temperatures are integrated, which allows to determine the evolution of the fluorescence signal as a function of temperature. In the case of FL and FL27, the integration was limited to the spectral region above 540 nm to avoid the errors caused by possible self-absorption at lower wavelengths. Taking as a reference $T_0 = 27$ °C, normalized evolutions of the fluorescence signal are plotted in Fig. 4 for all the dyes. Here also, a wide variety of behavior can be pointed out among the dyes, the most significant variations being observed for FL, RhB, and KR.

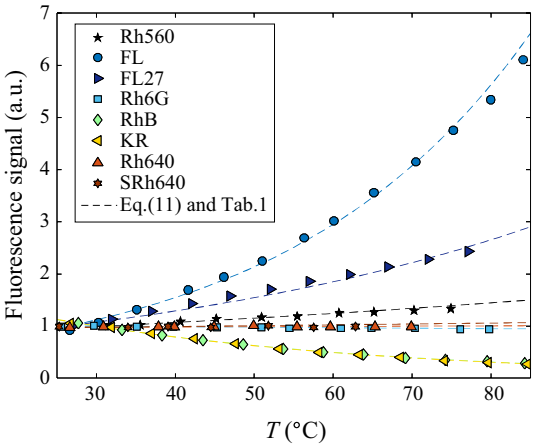

Fig. 4 Variation in the fluorescence signal as a function of the temperature taking as a reference $T_0 = 27$ °C (pH 5.6 in the case of FL)

In order to quantify the temperature dependence of the dyes' emission, the sensitivity coefficient s can be introduced. This parameter corresponds to the

relative temperature change in the fluorescence signal F, i.e., $s = \frac{1}{F}\frac{dF}{dt}$. If s does not vary with the temperature, the fluorescence signal can be expressed as:

$$F(T) = F(T_0)\exp\{s \cdot (T - T_0)\}, \tag{8}$$

where T_0 is an arbitrary temperature. Based on this expression, the temperature sensitivity s can be estimated from just two measurement points taken at temperatures T_0 and T_1:

$$s = \frac{\ln(F(T_1)/F(T_0))}{T_1 - T_0}. \tag{9}$$

This estimation of s will be all the more accurate than T_0 and T_1 are well separated. The values of s obtained by setting $T_0 = 27\,^{\circ}\mathrm{C}$ and $T_1 = 80\,^{\circ}\mathrm{C}$ are indicated in Table 1. The results of Eq. (8), taking for s the values displayed in Table 1, are presented in Fig. 4 with a dotted line. Equation (8) appears as a good approximation of the evolution of the fluorescence signal. This confirms that the temperature sensitivity s is nearly a constant for all the tested dyes. The comparative results presented in Table 1 and Fig. 4 deserve some comments:

- A marked decrease in the fluorescence with temperature is observed in the case of RhB and KR. The values obtained for the sensitivity coefficient s (about $-2.3\,\%/^{\circ}\mathrm{C}$) are comparable to those reported in previous studies such as Sakakibara and Adrian (1999) where the 514.5-nm line of an argon-ion laser was used to induce the fluorescence of RhB. Coppeta and Rogers (1998, Figs. 18 and 22) showed that the absorption coefficients of RhB and KR do not depend on the temperature, especially at 532 nm. The temperature dependence of the fluorescence signal is therefore exclusively the result of the decrease in the QY. The temperature dependence of the QY is well known and has been characterized in several solvents for RhB and KR (Kubin and Fletcher 1983).

Table 1 Variation in the fluorescence signal in the range (27−80 °C) for a laser excitation at 532 nm

	Sensitivity coefficient s defined in Eq. (9) (%/°C)
Rhodamine 560	+0.78
Fluorescein disodium at pH 5.6	+3.22
Fluorescein 27	+1.88
Rhodamine 6G	−0.07
Rhodamine B at pH 6.5	−2.38
Kiton red	−2.43
Rhodamine 640	+0.05
Sulforhodamine 640	−0.06

- Rh6G, Rh640, and SRh640 have a very low sensitivity to temperature. This observation is in line with previous studies. Coppeta and Rogers (1998) reported a variation in $+0.22\,\%/^{\circ}\mathrm{C}$ for SRh640 using an excitation at 514.5 nm. Saeki and Hart (2001) obtained $-0.1\,\%^{\circ}\mathrm{C}$ for Rh640 at 532 nm between 20 and 85 °C. These dyes have QYs of nearly 1 in water, EtOH and MeOH (Brouwer 2011; Kubin and Fletcher 1983). For Rh640, the QY was shown to be independent of temperature (Karstens and Kobs 1980). This insensitivity is caused by the rigid structure of the molecule: Almost no rotational degree of freedom is excited contrary to RhB or KR. At the same time, Rh6G, Rh640, and SRh640 have an absorption coefficient at 532 nm weakly affected by the temperature, as illustrated by Coppeta and Rogers (1998, Fig. 24) in the case of SRh640.
- For Rh560, FL and FL27, the fluorescence signal increases with temperature. Based on Eq. (7), it can be anticipated that this behavior is caused by an increase in the absorption cross section at 532 nm when the temperature increases. Sutton et al. (2008) have shown that the fluorescence signal of FL27 increases in the same proportion as the absorption coefficient at 532 nm, meaning that the QY is not influenced by the temperature. Coppeta and Rogers (1998) reported an effect of the temperature on the absorption coefficient of FL. They observed that ε increases with the temperature for $\lambda > 495$ nm while it decreases for $\lambda < 495$ nm. This certainly explains the differences in temperature sensitivities reported in the literature for FL. The coefficient s was evaluated at $-0.3\,\%/^{\circ}\mathrm{C}$ by Walker (1987) at $\lambda_{ex} = 488$ nm, while $+2.48\,\%/^{\circ}\mathrm{C}$ was obtained at $\lambda_{ex} = 514.5$ nm by Coppeta and Rogers (1998) and $+3.22\,\%/^{\circ}\mathrm{C}$ in the present study at $\lambda_{ex} = 532$ nm. Also, the absorption coefficient of FL is known to greatly increase with pH (Coppeta and Rogers 1998). Measurements taken with different pH buffers in the water solution reveal that the temperature dependence of ε at 532 nm is also the function of pH (Fig. 5). At pH 5.6, the comparison between the evolutions presented in Figs. 4 and 5 shows that the fluorescence signal of FL increases twice as much as its absorption coefficient at 532 nm between 27 and 80 °C, which cannot be explained by Eq. (7). This difference could be due to the existence of several protolytic forms of FL (anion, dianion, neutral, and cation). The two main protolytic forms of FL (anion and dianion) have quite different QYs (0.3 and 0.83, respectively) and absorption cross sections according to Sjöback et al. (1995). The equilibrium concentrations between the protolytic forms of FL, and thus the global QY and absorption coefficient of the dye molecules, are likely to change with temperature and pH.

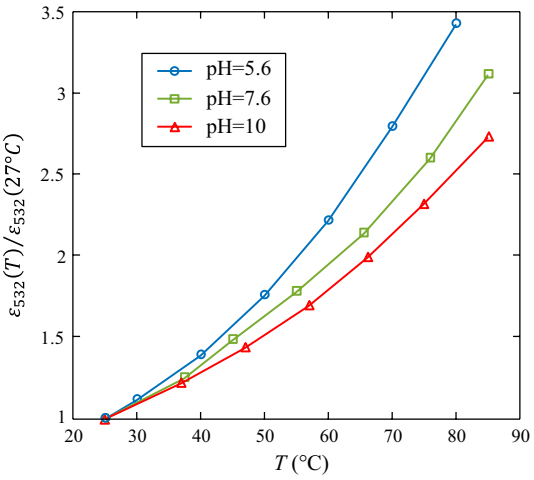

Fig. 5 Influence of the temperature on the absorption coefficient of FL at 532 nm taking as a reference $T_0 = 27\,°C$

Another important point to mention is that temperature sensitivity is generally wavelength-dependent. This property is exploited in an appropriate way in the 2c/1d method (Lavieille et al. 2000). For illustration, the sensitivity coefficient s was calculated for each wavelength composing the emission spectrum of the dyes using Eq. (9) by taking $T_0 = 27\,°C$ and $T_1 = 80\,°C$. The results displayed in Fig. 6 for RhB, KR, and SR640 reveal that the temperature sensitivity is significantly larger near the peak and the red-edge region of the emission spectrum. Difference in temperature sensitivity between the regions of the fluorescence spectrum can reach about 1.5 %/°C in the case of KR and RhB. Calculations are not reliable in the case of FL for the wavelengths below 540 nm, as these wavelengths are partially reabsorbed in a temperature-dependent way in the solution. It can be only concluded that the sensitivity s does not significantly vary above 540 nm.

3.2 Effect of laser irradiance

To study the effect of the laser irradiance I_0, the CW laser used in the previous measurements is replaced by a pulsed Nd:YAG laser at 532 nm (repetition rate: 15 Hz, pulse duration: 8 ns) whose pulse energies and average powers are measured by a pyroelectric sensor. Pulse energies over three decades (typically from a few tens of μJ to about 100 mJ) have been tested, while the temperature in the liquid cell is maintained at 25 °C. The fluorescence signal is measured using a spectrometer, which integrates during a few seconds the fluorescence signal generated by repeated laser pulses. As shown in Fig. 7, the fluorescence signal loses its proportionality to I_0 at high irradiances. The upper limit of the linear regime can be evaluated to a few 10^5 W/cm^2. As noted by Crimaldi (2008), a partial saturation of the fluorescence signal can be easily encountered in a typical light

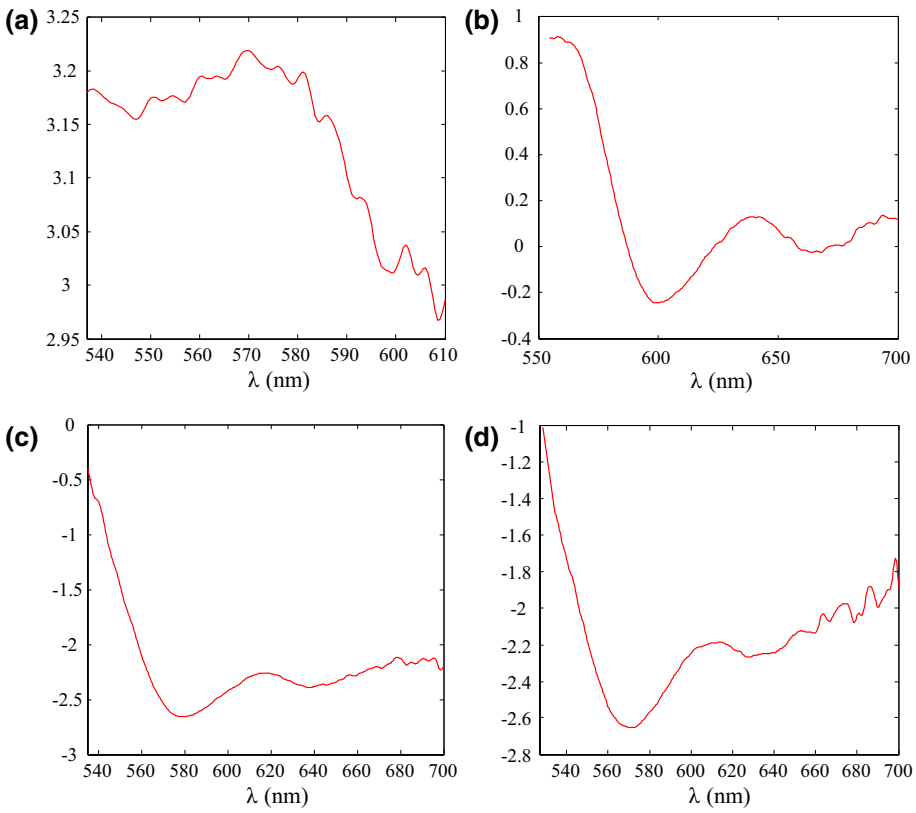

Fig. 6 Sensitivity to the temperature in %/°C of the fluorescence emission by wavelength (**a** FL at pH 5.6, **b** SRh640, **c** KR, **d** RhB)

sheet produced by a pulsed Nd:YAG laser. For example, under our experimental conditions (a laser sheet of thickness $e = 1$ mm and height $H = 2$ cm), energy of about 1 mJ is sufficient to produce a nonlinear response of the fluorescence. The selected dyes, namely FL, KR, RhB, and SRh640, have very similar responses to laser energy, which suggests they have about the same saturation intensity I_{sat}. A good agreement between Eq. (6) and the experiments is obtained by fixing $I_{sat} \approx 120 \times 10^5$ W/cm^2 as illustrated by the solid line displayed in Fig. 7a. Nonetheless, the estimation of I_{sat} may be affected by large errors as the dimensions of the laser beam were estimated from the burn pattern marked in a photosensitive paper. To evaluate the laser irradiance, the energy measured by the pyrometer is divided by the surface of the burn pattern and by the duration of the laser pulses assuming a uniform distribution of the energy inside the laser beam, but the latter is probably rather Gaussian.

In a second step, the variation in the fluorescence signal as a function of temperature was characterized at different pulse energies (Fig. 8). A marked decrease in temperature sensitivity can be observed in the case of RhB and KR

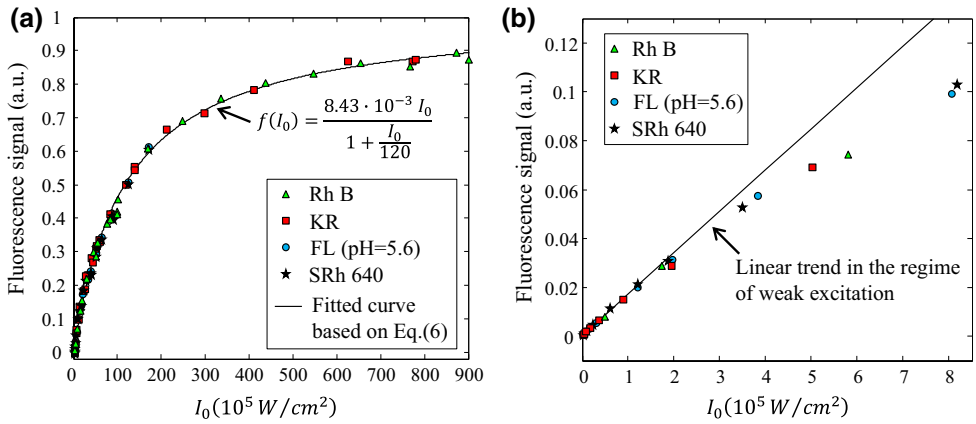

Fig. 7 Fluorescence signal as a function of the laser irradiance I_0

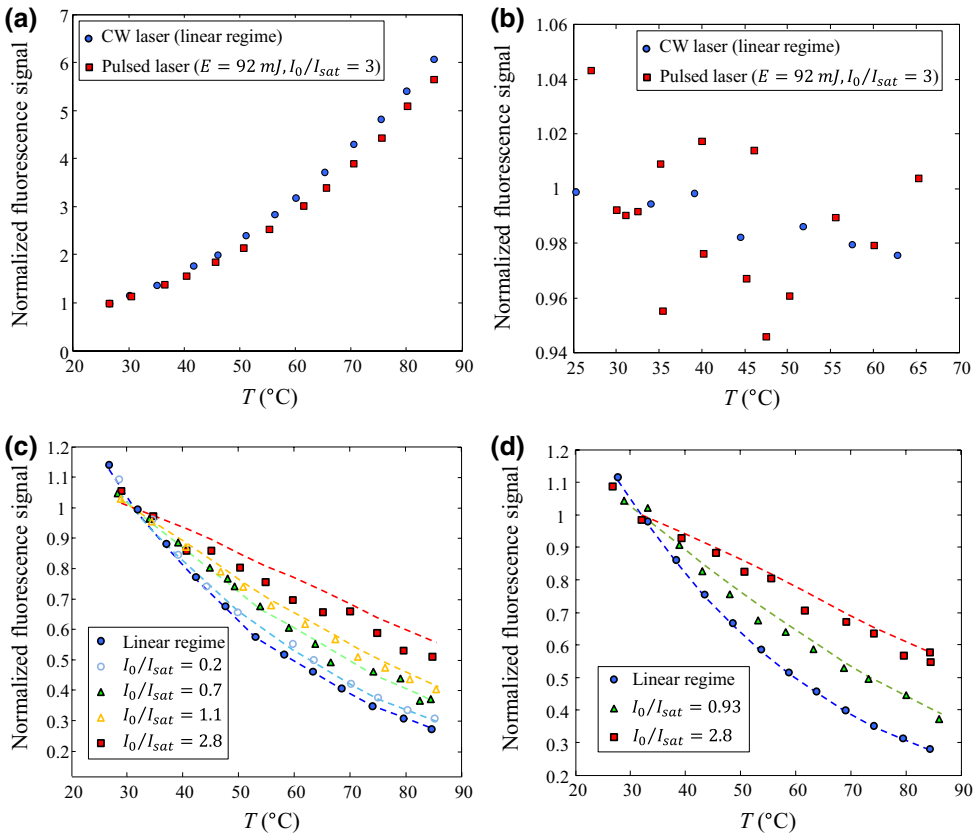

Fig. 8 Relative variation in the fluorescence signal with temperature (**a** FL, **b** SRh640, **c** KR, **d** RhB). In **c**, **d**, the dotted line corresponds to the application of the model Eq. (7) assuming $I_{sat} = 120 \times 10^5$ W/cm^2

when the pulse energy is increased (Fig. 8c, d). For pulse energies of about 80 mJ (corresponding to an intensity of about three times I_{sat}), sensitivity to temperature is about 40 % lower than in the linear regime of excitation. A good agreement can be obtained between the experimental data and Eq. (7) derived from the two-level model presented in Sect. 2. In the case of FL and SRh640, laser energy appears to have very little effect on the dependence of the signal to temperature. Only a very slight decrease in temperature sensitivity can be pointed out for FL in Fig. 8a. Also, the fluorescence of SRh640 remains quite insensitive to temperature at high laser irradiance. The scattering of the data in Fig. 8b is related to fluctuations in energy of the laser pulses during the measurements which are on the order of a few percents. Here also, the observations for FL and SRh640 agree well with Eq. (6), since the QY of FL and SRh640 are known to be temperature-independent. For these dyes, the expression of the fluorescence signal (Eq. 6) simplifies as $g_{\lambda,0}(T) \approx 1$ and the dependence to the ratio I_0/I_{sat} vanishes. As already mentioned, FL has an extra sensitivity to temperature that is not accounted for in Eq. (6) coming probably from its protolytic properties.

4 Quantitative measurements

One of the main difficulties for temperature measurement relates to the dependence of the fluorescence signal to many factors in addition to the temperature. Based on Eq. (6), the fluorescence signal is the function of the concentration in dye molecules C and the laser intensity I_0 in the measurement volume, which may differ from that at the exit of the laser due to the effect of the absorption in the liquid medium. The fluorescence emitted in the probed region of the flow can be also absorbed on its way to the detector. In practice, while concentration in dye molecules and laser emission can be made relatively stable during the experiments, the transmission of laser and fluorescent lights in the liquid flow can be very difficult to control. The problem cannot be solved by a normalization by a reference (acquired at a known temperature) given that the disturbances affecting the signal may differ between the reference and the measurements. In view of the results presented in Sect. 3, various solutions are tractable depending on the excitation regime of the fluorescence.

4.1 Linear regime of excitation by the laser

In the regime of weak excitation, the proportionality of the fluorescence signal to the laser irradiance allows ratiometric approaches. As already explained, several versions have been demonstrated in the past.

The 2c/2d approach made use of the ratio between the emission of two dyes having different sensitivities to temperature. One detection band should be dominated by the emission of the first dye and the other by that of the second dye. Among the dyes tested in Sect. 3, the couples FL/RhB and FL/KR are very attractive due to the opposite temperature sensitivities of the dyes involved in these couples. These dyes have also emission and absorption spectra that are well separated to limit the spectral conflicts (Sect. 5). Potentially, the temperature sensitivity could reach an impressive 5.7 %/°C. For some applications, this very high sensitivity compared to the literature could be a substantial improvement. It should be noted that Shafii et al. (2010) have already used the couple FL/KR to measure the temperature in aqueous solution. They reported a temperature sensitivity slightly smaller of the order of 4 %/°C. The difference with the current results is certainly caused by the pH fixed at 7.8 and the excitation wavelength set at 514.5 nm in their case.

An alternative for the measurements is the 2c/1d method, in which two spectral bands with different temperature sensitivity are selected in the emission spectrum of a single dye (Lavieille et al. 2000). The largest temperature sensitivities are achieved with KR and RhB (about 1.5 %/°C in Fig. 6c, d).

4.2 Saturated regime of excitation by the laser

The fluorescent signal becomes independent of the laser irradiance, when $I_0 \gg I_{sat}$. This property can be exploited for measuring the temperature using a one-color/one-dye (1c/1d) approach. A normalization of the fluorescence signal by a reference also taken in the saturated regime is enough to determine the temperature (provided that the transmission of fluorescence to the optics is not disturbed). For those measurements, using RhB or KR is not possible, since these dyes lose their temperature sensitivity in the saturated regime (Fig. 8). FL27 and FL are better candidates, provided they are resistant to photodegradation processes.

4.3 Partially saturated fluorescence

Most of the PLIF applications with pulsed lasers are in this intermediate situation where $I_0 \approx I_{sat}$, when the duration of the laser pulses is of the order of a few nanoseconds. From a rigorous point of view, the nonlinearity of the signal to the laser irradiance prohibits the use of ratiometric methods. However, since it is possible to find dyes with very similar saturation intensities, the 2c/2d approach can certainly be implemented with a minimum of error caused by the nonlinear dependence to laser irradiance. It can be anticipated that the pair FL/SRh640 will be well adapted for measurements, since both dyes have a temperature

sensitivity s which is not affected by I_0 (Fig. 8). The very sensitive pairs FL/KR and FL/RhB could be also an acceptable choice provided that the observation of the fluorescence field is restricted to a uniformly illuminated region of the flow and that the variations in energy of the laser pulses are small. A calibration performed exactly at the same irradiance as the measurements will be necessary to convert the signal ratio of the two detection bands into temperature, since KR and RhB have a temperature sensitivity depending on I_0 (Fig. 8).

Measuring the fluorescence lifetime in order to determine the temperature is an interesting alternative to the above-described approaches based on the signal intensity. Molecules having a temperature-dependent QY also have a fluorescence lifetime that depends on the temperature (Sect. 2). The great advantage of lifetime measurement techniques is their inherent independence to the intensity of the laser excitation. Molecules with a long-lived phosphorescence (on the order of a few ms) allow relatively easy measurements of the lifetime. A conventional camera operating in PIV mode can be used to characterize the phosphorescence decay in the molecular tagging thermometry (MTT) developed by Hu et al. (2006). This approach, however, has its limitations. The time response of the technique is fixed by the phosphorescence lifetime and cannot be shortened too much if rapid events are to be studied. The temperature can be also determined based on lifetime measurements using thermographic phosphors in the form of nanopowders (Aldén et al. 2011).

5 Selection of the spectral bands

5.1 Spectral conflicts

The spectral bands of detection have been selected in order to avoid spectral conflicts (or overlaps between absorption and emission bands), which are known to affect negatively the accuracy and the implementation of the measurements (Coppeta and Rogers 1998; Sakakibara and Adrian 1999). In practice, different spectral conflicts can be encountered:

- *Type I* Due to an overlap between the emission bands of the dyes, some of the fluorescence from one dye appears in the intensity measurement of the other dye. This situation has been addressed by Sakakibara and Adrian (1999) and is known to result in a reduced accuracy in temperature measurements. Moreover, the temperature sensitivity becomes dependent on the ratio of dye concentrations which has therefore to be absolutely maintained constant and uniform during the experiments.
- *Type II* Due to an overlap between the emission band of one dye and the absorption band of the same dye or the other one, the fluorescence is partially absorbed. For conflicts of type II, the absorption coefficient of the absorbing dye must not depend on temperature and its concentration must be constant and uniform in the medium. As a result of a conflict of type II, the signal ratio of the two detection bands becomes dependent on the location of the measurement volume given that absorption is function of the path length between the laser excited zone and the fluorescence detector. This type of conflict can be corrected by a normalization of the fluorescence ratio by a reference taken at the same path length.
- *Type III* As for the type II conflict, the fluorescence detected on a spectral bands is absorbed. However, the absorption coefficient depends on the temperature which is not uniform in the liquid medium. Measurement errors cannot be corrected through a normalization (as for type II conflicts) because the absorption is a function of an undetermined temperature field. Therefore, conflict of type III must be avoided as much as possible.

5.2 Detection bands

- *Detection bands using the 2c/2d method* The couple FL/SRh640 will be tested for measuring the temperature in the conditions of a partially saturated fluorescence. Based on the previous discussion, it was decided to use for the detection of the fluorescence signal, the bands (540–560 nm) and (630–650 nm). The absorption of SRh640 being not dependent on temperature (Coppeta and Rogers 1998), only a conflict of type II will affect the measurements. In the following, the low absorption efficiency of FL at 532 nm will be compensated by an increased concentration of FL. Therefore, it is very important to pay attention to the problem of the fluorescence reabsorption by FL. The risk of conflict of type III due to the temperature dependence of FL's absorption seems to be limited given that the detection is made above 540 nm.
- *Detection bands using the 2c/1d method* The effect of laser irradiance will be also assessed for the 2c/1d method selecting KR as the temperature-sensitive dye. For a high temperature sensitivity, the best choice is a narrow band centered around 540 nm and a second band above 570 nm (Fig. 6c). However, the risk is to have very little signal on the first detection band around 540 nm. A compromise should be made between signal and temperature sensitivity of the fluorescence ratio. The retained spectral bands correspond to (540–550 nm) and (630–650 nm). The band (540–550 nm) is prone to a conflict of type II given the absorption of KR below 610 nm (Fig. 2a). Furthermore, Lavieille et al. (2004)

demonstrated that the temperature sensitivity of the fluorescence ratio can be affected by the absorption of the fluorescence if the temperature dependence of the fluorescence signal strongly varies over the reabsorbed spectral band of detection. Presently, this effect is significant given the large variation in temperature sensitivity observed for KR between 540 and 580 nm (Fig. 6c). To limit the measurement errors, the calibration in temperature of the fluorescence ratio is performed at the same optical depth as the measurements. This problem can be safely ignored for the pair FL/SRh640, given that the temperature sensitivity of FL does not vary with the wavelength between 540 and 560 nm (Fig. 6a).

6 Measurement system

The measurement system is presented in Fig. 9. A pulsed frequency-doubled Nd:YAG laser at 532 nm is used for inducing the fluorescence of the dyes. The laser has a repetition rate of 10 Hz, and it can deliver pulse energies up to 150 mJ. A laser sheet is formed by means of a set of spherical and cylindrical lenses. Two intensified CCD cameras from Princeton Instruments (PI-MAX2 1003HB-43-filmless, 1024×1024 pixels) allow visualizing the fluorescence field in the probed region of the flow. A beam splitter tilted at 45 ° to the axis of the cameras allows having exactly the same field of view with the cameras. Band-pass interference filters (OD of 6 in the cutoff regions) are mounted on the objectives of the cameras to detect the fluorescence corresponding to the selected spectral bands (Sect. 5). The image acquisition is synchronized with the Q-switch signal of the laser cavity, while the signal integration by the cameras is set to cover a period of time (typically 40 ns) much longer than the duration of the laser pulses. A few percents of the laser beam are deviated for measuring the energy of the laser pulses and controlling its shot-to-shot fluctuations. To measure temperature fields, the dark noise

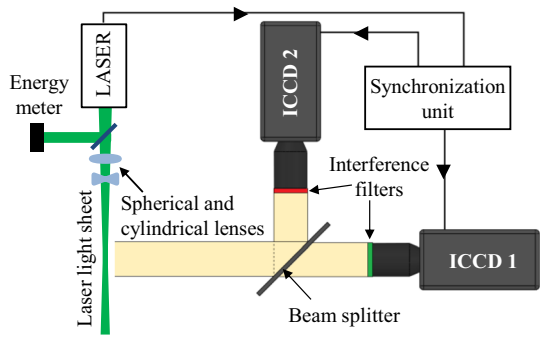

Fig. 9 Optical layout of the imaging system used for measuring the temperature

is first subtracted from the images recorded by both cameras, and then the fluorescence images are divided one by the other to calculate the signal ratio of the detection bands. The fluorescence ratio is then normalized by a reference ratio taken at an already-known temperature and the same optical path (as justified for type II conflict in Sect. 5). The normalized ratio is finally converted into temperature with the use of a calibration.

Several critical points must be considered before making measurements:

- Cameras may not have exactly the same field of view.
- The response of the camera to the incoming photons flux may not be linear and must be corrected.
- The signal-to-noise ratio will depend on the acquisition settings especially the gain of amplification of the ICCD cameras.

6.1 Pixel correspondence between the images of the cameras

To ensure that the two cameras can actually visualize the same spatial region, identical lenses are mounted in front of the cameras (Fig. 9). An equally spaced grid pattern at a few millimeter intervals is placed in front of the cameras. This grid plate is first tilted at 45 °, and the position of the cameras is adjusted to have the focus in the same central region of the image. An offset of a few pixels between the images of the two cameras may remain after this operation. For this reason, a calibration of the image coordinates is also performed following a procedure equivalent to that described by Sakakibara and Adrian (1999, 2004). The same grid pattern, now perfectly in focus, is tilted perpendicularly to the optical axis of the cameras. Then, a recognition algorithm is used to find the coordinates of each point of the grid in the images of the cameras. A 3rd order polynomial function is then created to obtain a perfect correspondence between the coordinates of the points in the images of the cameras. This polynomial function will be applied to all the images taken by the cameras during the experiments.

6.2 Linearity of the detection chain

Saturation effects in the microchannel plates (MCP) of ICCD cameras are known to occur with high-level input signals. They can be a major issue for quantitative measurements based on light intensity (Lindén et al. 2012). The camera response to light irradiance was therefore characterized for different amplification gains (i.e., different voltages applied between the input and the output of the MCP). The method implemented to determine the nonlinear response of the cameras consists to move a stepped neutral density in front of the cameras while taking images of

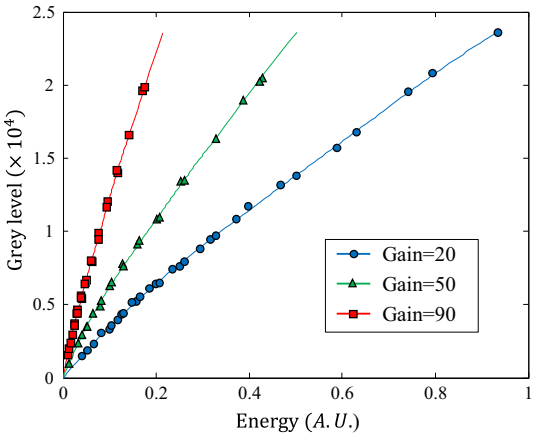

Fig. 10 Response of ICCD cameras to light irradiance

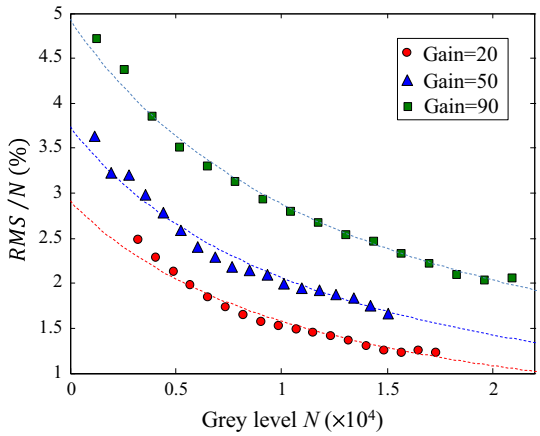

Fig. 11 Inverse of the signal-to-noise ratio of the camera at several gains of amplification. Dotted lines correspond to the fitting of the experimental data by a function of type $y(x) = a/(x + b)$, where a and b are two fitted parameters

the fluorescence of a dye at a fixed laser energy. Results of the calibration are displayed in Fig. 10. The abscissa corresponds to the received light energy (this quantity is known to be inversely proportional to the attenuation factor of the optical density placed in front of the camera) and in ordinate is the averaged level of the pixels. Figure 10 shows that the camera response to the light flux is not linear. In the following, Fig. 10 will serve to correct the nonlinearity of the ICCD cameras. Saturation effects in the MCP and the phosphor screen become significant above a gray level of about 25,000 at the low amplification gains used in the experiments to limit the measurement noise (Sect. 6.3). It was therefore decided not to exceed this threshold.

6.3 Signal-to-noise ratio and measurement uncertainties

A particular attention should be also paid to the signal-to-noise ratio of the cameras. Figure 11 shows the relative standard deviation of the pixels (i.e., the inverse of the signal-to-noise ratio) as a function of the average signal N. This figure is used to evaluate the uncertainty in the measurements. Given that there is no simple way to assess the RMS of the ratio between two randomly distributed variables, a general method using generators of random numbers is applied to evaluate how errors due to the camera noise propagate to the fluorescence ratio and the temperature. The procedure can be described as follows:

Step 1 Denoting I_1 and I_2 the signal levels measured by the cameras, the random noise associated with these level values is evaluated using Fig. 11.

Step 2 A generator of random numbers is used to create two series of 100,000 numbers following a normal distribution. The mean values of these series are, respectively, I_1 and I_2 and their standard deviations are those determine previously from Fig. 11.

Step 3 Gray levels are corrected from the nonlinearity of the camera response using Fig. 10. For that, each value of the series is replaced by its energy in abscissa of Fig. 10. Two series denoted I_1^* and I_2^* are obtained after that correction.

Step 4 The fluorescence ratio is calculated for each couple of numbers present in I_1^* and I_2^*, then the RMS of the fluorescence ratio I_1^*/I_2^* is evaluated.

Step 5 Finally, the uncertainty on the temperature measurement is obtained by dividing the RMS of the fluorescence ratio by the temperature sensitivity s known from a calibration in temperature.In order to assess the feasibility of an instantaneous measurement of the temperature (i.e., using a single laser shot), a rough estimate of the system performances can be obtained using the previously described method for uncertainty propagation. Assuming a signal of the order of 10,000 levels and a amplification gain of 20 for the ICCD cameras, the relative standard deviation of the fluorescence ratio can be evaluated at about 2.3 % if the responses of the cameras were linear (i.e., skipping step 3 in the above calculation). The uncertainty of the fluorescence ratio rises to 2.7 % if the nonlinearity of the cameras' response is accounted for. This value remains smaller than the temperature sensitivity of about 3 %/°C expected for the pair of dyes FL/SRh640 (Table 1). To measure the temperature instantaneously with about 1 °C of uncertainty, the challenge will be to approach the conditions of this calculation in the experiments.

7 Application to turbulent heated jets

The experimental configuration, chosen to test the feasibility of instantaneous temperature measurements, is similar to that studied by Bruchhausen et al. (2005). It consists in the observation of the thermal mixing in a turbulent water jet. This relatively well-known flow configuration will be used to analyze the sources of errors and uncertainties attached to instantaneous measurements of temperature fields. The experimental setup is shown in Fig. 12. Preheated water is injected into a large tank of dimensions 60 cm × 40 cm × 40 cm. The orifice of the injection nozzle has a diameter of 3 mm. A thermocouple is inserted into the nozzle to control the temperature of the injected water. The nozzle is placed at a distance $z = 5$ cm from the edge of the water tank, z being oriented perpendicular to the laser sheet. The injection flow rate is about 1.2 L/min, which allows achieving Reynolds numbers of the order of 10^4, well in the turbulent regime. The average temperature in the tank is little affected by the injection of hot water due the smallness of the injected volume over the duration of the measurements (typically one or two minutes). Nevertheless, a system of temperature regulation is used to limit the variation in the temperature. The injection system operates in a closed loop. A few liters of water are collected in the tank between two sets of measurement and heated to serve for the injection in the next set of measurements. A mirror inclined at 45 ° is used to illuminate the turbulent jet from below. The laser sheet is approximately 1.5 mm thick and 10 cm large in the region of the measurements. The cameras visualize a region of about 5 cm × 5 cm, and the spatial resolution is 0.5 × 0.5 mm^2. The temporal resolution is on the order of 7 ns, i.e., the duration of the laser pulses (5 ns) plus the fluorescence lifetime of the dyes (about 2 ns).

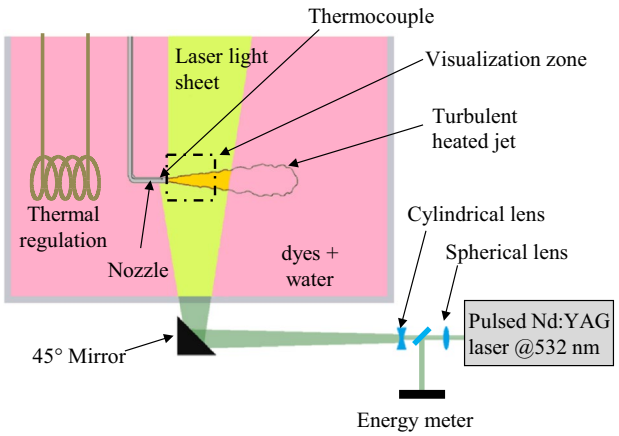

Fig. 12 Experimental setup used to study the turbulent mixing in a liquid jet

7.1 Temperature measurement with the 2c/1d method

Reliable measurements proved to be very difficult to obtain without averaging images. The main limitations come from the weakness of the signal collect on the (540–550 nm) band compared to the (630–650 nm) band. In the experiments, the concentration of KR was fixed at 3.3×10^{-7}mol/L while the energy of the laser pulse was 70 mJ (about 12 MW/cm^2). It was necessary to increase the gain of the cameras to have enough signals for the measurements. The gain was fixed at 90 for the band (540–550 nm) and 50 for the band (630–650 nm). Even so, the signal of the 1st detection band is much lower than that of the 2nd band as it can be observed in Fig. 13a, b (typically about 2000 levels against 7000 levels). In Fig. 13c, the instantaneous temperature field obtained from a single laser shot appears very noisy. Measurement uncertainties were determined from the signal-to-noise ratio of the cameras (Fig. 11). Estimation yields about 8 °C for the uncertainties in temperature. An average of about one hundred images is therefore required to achieve 1 °C of accuracy (Fig. 13d). Bruchhausen et al. (2005) also performed one-shot measurements of the temperature in turbulent jets using the 2c/1d method and RhB as temperature-sensitive fluorescence dye. Measured instantaneous temperature fields appear somewhat less noisy, and the turbulence structures are also more recognizable in this study (Bruchhausen et al. 2005, Fig. 11). In fact, a major difference compared to our measurements is that the cameras were operated in a 4-by-4 binning mode with a higher magnification lens to compensate for the loss of spatial resolution accompanying the binning. Performing a similar spatial averaging between neighbor pixels in our measurements would allow reducing the random noise and obtaining a comparable level of accuracy. Nevertheless, the instantaneous temperature measurements reported by Bruchhausen et al. (2005) are still far from 1 °C of accuracy. Increasing the concentration of KR could also help improving the measurement accuracy. However, the effects of laser absorption and fluorescence reabsorption have to be considered carefully. Calculations taking into account the extinction of the laser light and the fluorescence in the conditions of the experiments show that the signal of the 1st detection band could be increased by a factor two in the best case by increasing the dye concentration. However, this alone would be insufficient to achieve instantaneous temperature measurements with approximately 1 °C of accuracy. Increasing the energy of the laser pulses is also a possibility, but the decrease in temperature sensitivity with the laser energy will be detrimental (Fig. 14).

Otherwise, it should be emphasized that the nonuniformity of the laser excitation was not taken into account in the conversion of the fluorescence ratio into temperature

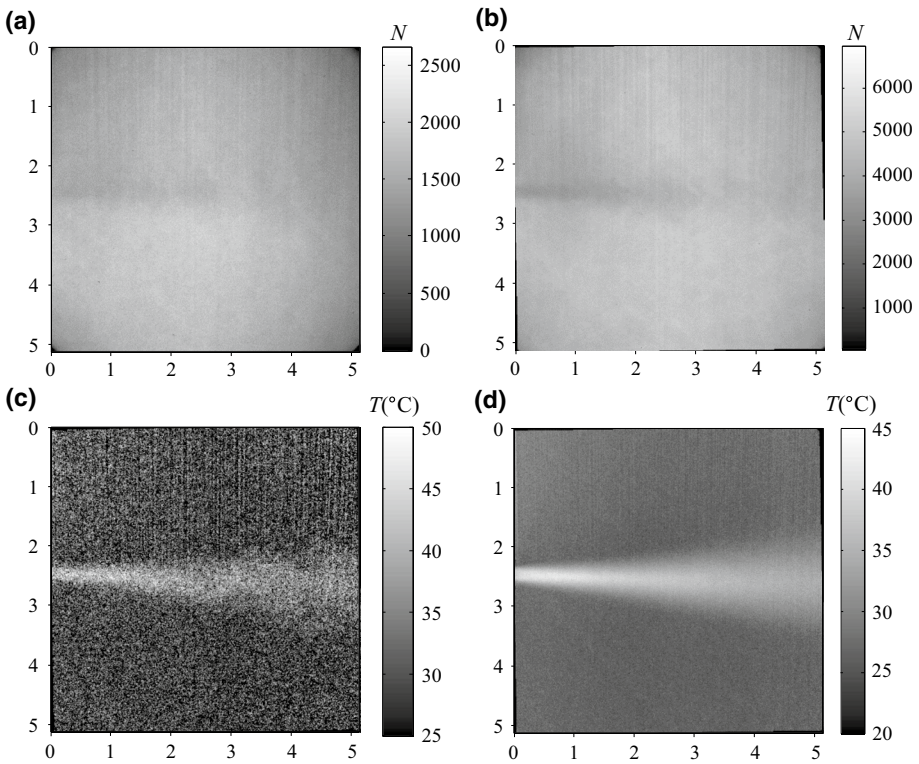

Fig. 13 Typical experimental results obtained with the 2c/1d method [**a**, **b** raw images of the fluorescence detected on the bands (540–550 nm) and (630–650 nm), **c** instantaneous temperature measurements, **d** average temperature determined from 200 pairs of images]. The *scale* unit of the image is 1 cm

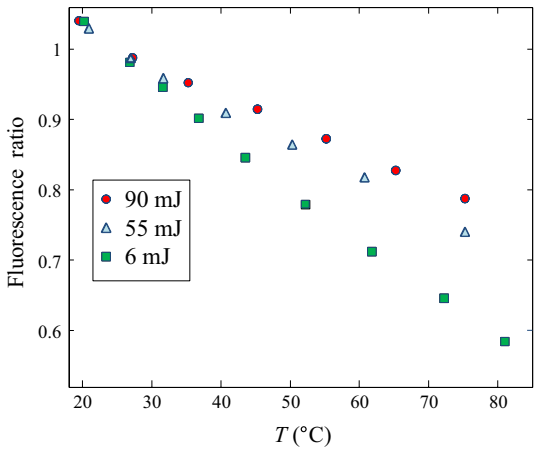

Fig. 14 Influence of the energy of the laser pulses on the temperature dependence of the fluorescence ratio in the application of the 2c/1d method with KR

in Fig. 13c, d. As the temperature sensitivity of the fluorescent ratio varies with the laser irradiance that is a priori not uniform, temperature measurements are biased and cannot be corrected.

7.2 Temperature measurement with the 2c/2d method

The same experiment was carried out using the 2c/2d approach with the couple of dyes FL/SRh640. The energy of the laser pulses is fixed at 90 mJ corresponding to a laser irradiance of 18 MW/cm^2, while the dye concentrations are $C(\text{SRh640}) = 7.74 \times 10^{-7}$ mol/L and $C(\text{FL}) = 5 \times 10^{-5}$ mol/L. The much higher concentration of FL is necessary to compensate for the very low absorption of FL at 532 nm and its absorption by SRh640, the injection nozzle being positioned at an optical depth $z = 5$ cm. The chosen ratio between the concentrations of FL and SRh640 allows having about the same signal on the two cameras while observing the laser sheet at $z = 5$ cm for a liquid temperature of 22 °C. Due to the aforementioned pH sensitivity of FL, pH was stabilized at 5.6 adding 4.7 mg/L of disodium hydrogen phosphate (Na_2HPO_4) and 83 mg/L of potassium dihydrogen phosphate (KH_2PO_4). The temperature coefficient of phosphate buffers is $-0.0028\,\text{K}^{-1}$; thus, pH should very weakly depend on the temperature in the experiment. In these experimental conditions, both ICCD cameras could operate with a relatively low gain of 20, which considerably limits the noise.

A typical pair of images recorded on both cameras is shown in Fig. 15a, b. Signal levels exceed about 8000 levels on these two images, which appears to be acceptable to measure the temperature instantaneously. Indeed, much less noise is present in the instantaneous temperature field derived from these images (Fig. 15c) compared to the previous measurements obtained using KR alone (Fig. 13c). While an absence of temperature sensitivity was expected for SRh640, the fluorescence signal is slightly higher in

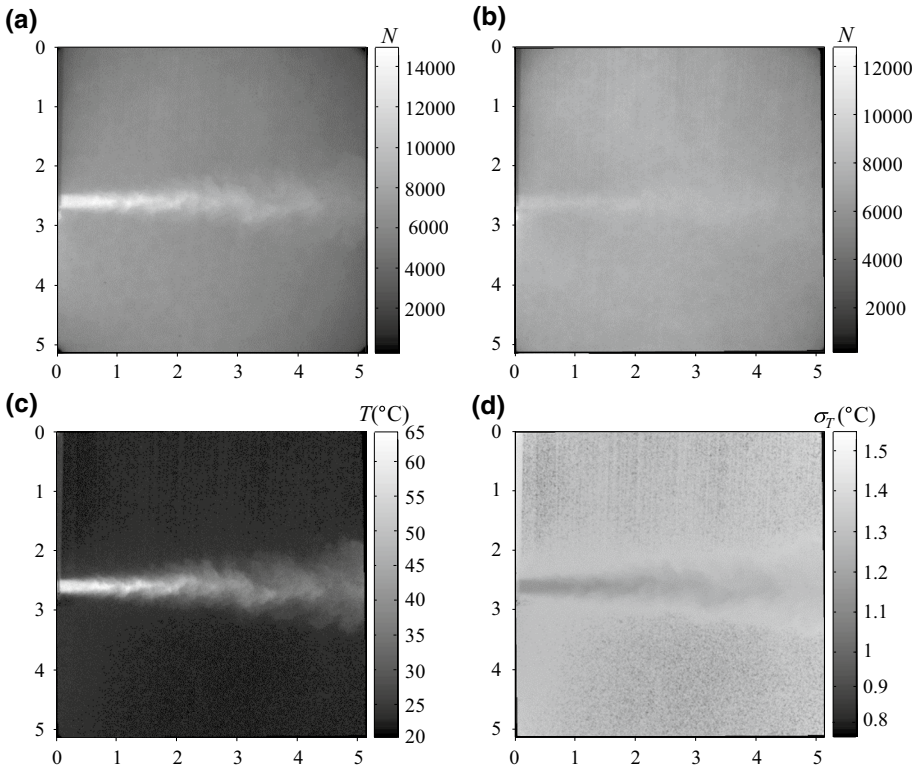

Fig. 15 Typical experimental results obtained with the 2c/2d method [**a**, **b** raw images of the fluorescence detected on the bands (540–560 nm) and (630–650 nm), **c** instantaneous temperature measurements, **d** estimated uncertainties on the temperature measurements]. The *scale* unit of the image is 1 cm

the turbulent jet region in Fig. 15b which shows the fluorescence detected on the band (630–650 nm) is dominated by the SRh640 emission. This small increase may originate from two factors. First, even if SRh640 is globally insensitive to the temperature (Table 1), some spectral regions of its emission spectrum can have slight temperature dependences. A small increase in the SRh640 emission with the temperature (about $+0.1\,\%/°C$) can be observed around 640 nm in Fig. 6b. Secondly, it is possible that FL has a small contribution to the signal detected in the band (630–650 nm). In Fig. 2b, the upper limit of the emission spectrum of FL appears to be close to 640 nm according to the measurements by the spectrometer.

Given that Fig. 15a, b corresponds to raw images, which are not corrected for the nonlinearity of the ICCD sensor (Fig. 10), the range of variations in the fluorescence signal emitted by FL (between 14000 and 8000 levels for temperatures ranging from 20 to 65 °C) appears much more limited than expected according to Fig. 6a. Fig. 16 shows the calibration curve (the one at $z = 5$ cm) used to determine the temperatures displayed in Fig. 15c. This calibration, carried out in a uniformly heated cell, is used to convert the ratio of the fluorescence images into temperature after correction of the nonlinearity of the camera responses and a normalization of the images by reference images recorded without a turbulent jet. A comparison with another calibration performed at $z = 3$ mm reveals a loss of temperature sensitivity with the depth

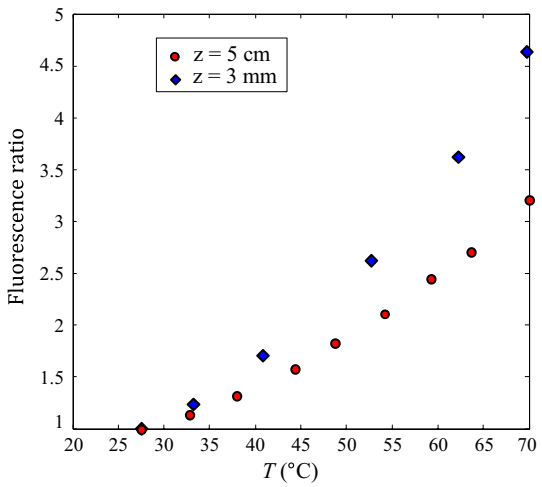

Fig. 16 Variation in the fluorescence ratio with the temperature for two optical depths

position of the measurements in the liquid solution. The temperature dependence is about $+3\,\%/°C$ at $z = 3$ mm (well in line with Figs. 6a and 8a) against $+2.5\,\%/°C$ at $z = 5$ cm over the temperature range 25–65 °C. The most probable hypothesis to explain this loss of sensitivity is an absorption by FL of its own emission in the (540–560 nm) region, which would correspond to a conflict of type III (Sect. 5.1). Nevertheless, this explanation is not totally satisfying given the low values obtained for the absorption

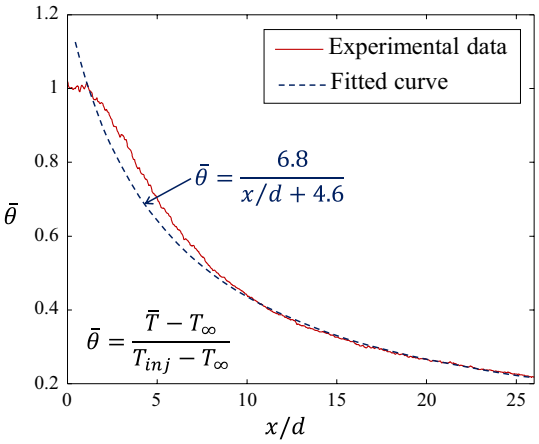

Fig. 17 Evolution of the normalized mean temperature $\overline{\theta}$ along the centerline of the turbulent jet. $\overline{T}$ is the time-averaged temperature, x/d is the reduced distance to the injector with d the diameter of the injection nozzle. ($d = 3$ mm, $T_{\text{inj}} = 63\,^{\circ}\text{C}$ and $T_\infty = 22\,^{\circ}\text{C}$)

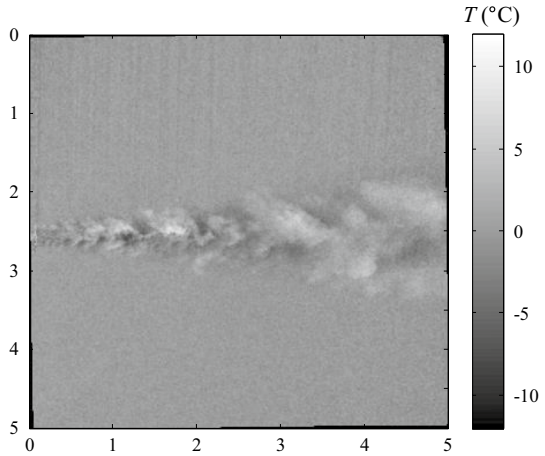

Fig. 18 Typical instantaneous temperature fluctuations measured in the turbulent heated jet. This image is obtained by subtracting the average temperature derived from two hundreds of images to the instantaneous temperature field in Fig. 15c

coefficient of FL in Fig. 2a. Further investigations are necessary to clearly understand the phenomenon. If a type III conflict is actually present, the resulting measurement bias cannot be corrected easily, as temperature is not distributed uniformly inside the turbulent jet unlike in the calibration cell.

Here also, the temporally averaged temperature $\overline{T}$ was determined using 200 pairs of images. The evolution of the mean temperature along the centerline of the turbulent jet is presented in Fig. 17. The streamwise decay of the temperature follows a usual hyperbolic law. For instance, the constant 6.8 at the numerator of the equation of the fitted curve is comparable to that obtained by Antoine et al. (2001).

The propagation method described in Sect. 6.3 was used to estimate the measurement uncertainties. Calculations are based on the levels of the raw images (Fig. 15a, b) and the temperature calibration at $z = 5$ cm (Fig. 16). Despite a temperature sensitivity slightly lower than expected, uncertainties are of the order of 1.2 °C in the central zone of the turbulent jet and 1.5 °C in the outside of the jet. These values were obtained taking into account the nonlinear response of the ICCD cameras which is responsible for a further reduction in the measurement accuracy. The uncertainties of the temperature measurements are rather small compared to the temperature fluctuations in the jet (Fig. 18) which are determined by subtracting the instantaneous temperature field in Fig. 15c by the average temperature obtained from the sum of two hundreds of images. It can be therefore anticipated that these measurements are accurate enough to allow a fine investigation of the turbulence characteristics of the flow. Nevertheless, measurement capabilities are limited by the relatively low repetition rate of the pulsed Nd:YAG laser and acquisition rate of the ICCD cameras.

8 Conclusion

In the ratiometric methods developed for measuring the temperature in the liquids, assumption of a proportionality between the fluorescence signal and the laser irradiance is generally made. When this assumption is verified (which is almost always the case with CW lasers), the fluorescence ratio allows to eliminate totally the effects of the laser intensity. The relevance of ratiometric approaches is thus fully justified for measurements taken under experimental conditions where the laser irradiance cannot be controlled. When pulsed lasers are used for the excitation of the fluorescence, their irradiance usually exceeds the saturation intensity of common fluorescent dyes. Therefore, the fluorescence signal loses its linear dependence on the laser irradiance. The results obtained in the present study show that this loss of linearity is not necessarily an important source of error for the ratiometric methods, because many dyes among the fluoresceins and the rhodamines have comparable saturation intensities.

However, for some dyes such as rhodamine B and Kiton red, the saturation of the fluorescence signal at high laser irradiances is accompanied by a significant loss of temperature sensitivity. The dyes, for which this loss of sensitivity is observed, mainly owe their temperature dependence to the fluorescence quantum yield and have a fluorescence signal decreasing with the temperature. A particular attention should be paid to this issue, since the gain of signal obtained using high excitation energies can be outweighed by the loss of temperature sensitivity. It is also necessary to calibrate the temperature response at the same laser irradiance than in the experiments when the measurements are taken in the partially saturated regime of excitation of the

fluorescence. Nevertheless, a measurement bias may exist if the excitation energy significantly varies within the laser sheet or during the experiments.

The same problem is not encountered with dyes whose temperature dependence originates from the variation in the absorption cross section. An interesting case is that of fluorescein excited at 532 nm which retains its high temperature dependency at high laser irradiances. In addition, some dyes such as sulforhodamine 640 keep their insensitivity to the temperature in the linear and saturated regimes of excitation. Thus, the couple fluorescein/sulforhodamine 640 can be proposed for an implementation of the ratiometric method without any significant risk of errors at high laser irradiance. Also, the high temperature dependence of the fluorescein signal (about $+3\,\%/°\mathrm{C}$) can be utilized to measure instantaneous temperature fields. The main drawback with this couple of dyes is the high concentrations of fluorescein required to obtain a signal comparable to that of sulforhodamine 640. This is due to the low absorption cross section of the fluorescein disodium at 532 nm. Because of the high concentration of fluorescein, reabsorption can be a problem for an implementation of the technique in liquid media with relatively large optical thickness. The insensitivity of the couple fluorescein/sulforhodamine 640 to the laser irradiance, both in the partially saturated and saturated regimes of excitation, is a very interesting feature for application of planar applications of the two-color LIF thermometry in multiphase flows (sprays, wavy liquid films, bubbly flows,...), where liquid–gas interfaces can lead to highly inhomogeneous distributions of excitation energy in the liquid phase.

References

Aldén M, Omrane A, Richter M, Särner G (2011) Thermographic phosphors for thermometry: a survey of combustion applications. Prog Energy Combust Sci 37(4):422–461

Antoine Y, Lemoine F, Lebouché M (2001) Turbulent transport of a passive scalar in a round jet discharging into a co-flowing stream. Eur J Mech B/Fluids 20(2):275–301

Brouwer AM (2011) Standards for photoluminescence quantum yield measurements in solution (iupac technical report). Pure Appl Chem 83(13):2213–2228

Bruchhausen M, Guillard F, Lemoine F (2005) Instantaneous measurement of two-dimensional temperature distributions by means of two-color planar laser induced fluorescence (plif). Exp Fluids 38(1):123–131

Castanet G, Labergue A, Lemoine F (2011) Internal temperature distributions of interacting and vaporizing droplets. Int J Therm Sci 50(7):1181–1190

Coolen M, Kieft R, Rindt C, van Steenhoven A (1999) Application of 2-d lif temperature measurements in water using a nd : Yag laser. Exp Fluids 27(5):420–426

Coppeta J, Rogers C (1998) Dual emission laser induced fluorescence for direct planar scalar behavior measurements. Exp Fluids 25(1):1–15

Crimaldi J (2008) Planar laser induced fluorescence in aqueous flows. Exp Fluids 44(6):851–863

Dunand P, Castanet G, Lemoine F (2012) A two-color planar lif technique to map the temperature of droplets impinging onto a heated wall. Exp Fluids 52(4):843–856

Düwel I, Schorr J, Wolfrum J, Schulz C (2004) Laser-induced fluorescence of tracers dissolved in evaporating droplets. Appl Phys B 78(2):127–131

Hishida K, Sakakibara J (2000) Combined planar laser-induced fluorescence-particle image velocimetry technique for velocity and temperature fields. Exp Fluids 29(1):S129–S140

Hu H, Koochesfahani M, Lum C (2006) Molecular tagging thermometry with adjustable temperature sensitivity. Exp Fluids 40(5):753–763

Karstens T, Kobs K (1980) Rhodamine b and rhodamine 101 as reference substances for fluorescence quantum yield measurements. J Phys Chem 84(14):1871–1872

Kim M, Yoda M (2010) Dual-tracer fluorescence thermometry measurements in a heated channel. Exp Fluids 49(1):257–266

Kubin R, Fletcher A (1983) Fluorescence quantum yields of some rhodamine dyes. J Lumin 27(4):455–462

Labergue A, Delconte A, Lemoine F (2013) Study of the thermal mixing between two non-isothermal sprays using combined three-color lif thermometry and phase doppler analyzer. Exp Fluids 54(6)

Lavieille P, Lemoine F, Lebouché M (2000) Sur l'utilisation de traceurs fluorescents pour mesurer la température de gouttelettes. Comptes Rendus de l'Académie des Sciences Series IIB Mech Phys Astron 328(1):55–60

Lavieille P, Delconte A, Blondel D, Lebouche M, Lemoine F (2004) Non-intrusive temperature measurements using three-color laser-induced fluorescence. Exp Fluids 36(5):706–716

Lee TW (2008) Thermal and flow measurements. CRC Press, Boca Raton

Lemoine F, Castanet G (2013) Temperature and chemical composition of droplets by optical measurement techniques: a state-of-the-art review. Exp Fluids 54(7)

Lemoine F, Antoine Y, Wolff M, Lebouche M (1999) Simultaneous temperature and 2d velocity measurements in a turbulent heated jet using combined laser-induced fluorescence and lda. Exp Fluids 26(4):315–323

Lindén J, Knappe C, Richter M, Aldén M (2012) Limitations of iccd detectors and optimized 2d phosphor thermometry. Meas Sci Technol 23(3):035,201

Melton L, Lipp C (2003) Criteria for quantitative plif experiments using high-power lasers. Exp Fluids 35(4):310–316

Nakajima T, Utsunomiya M, Ikeda Y, Matsumoto R (1990) Simultaneous measurement of velocity and temperature of water using LDV and fluorescence technique. In: Fifth international symposium on applications of laser techniques to fluid mechanics, Lisbon, Portugal

Natrajan VK, Christensen KT (2009) Two-color laser-induced fluorescent thermometry for microfluidic systems. Meas Sci Technol 20(1):015,401

Saeki S, Hart D (2001) Investigation on yag (532) laser dyes for oil film thickness and temperature measurement. In: Proceedings of the third pacific symposium of flow visualization and image processing, Maui, Hawaii, p Paper index number F3096

Sakakibara J, Adrian R (1999) Whole field measurement of temperature in water using two-color laser induced fluorescence. Exp Fluids 26(1–2):7–15

Sakakibara J, Adrian R (2004) Measurement of temperature field of a Rayleigh–Benard convection using two-color laser-induced fluorescence. Exp Fluids 37(3):331–340

Sakakibara J, Hishida K, Maeda M (1993) Measurements of thermally stratified pipe-flow using image-processing techniques. Exp Fluids 16(2):82–96

Shafii M, Lum C, Koochesfahani M (2010) In situ lif temperature measurements in aqueous ammonium chloride solution during uni-directional solidification. Exp Fluids 48(4):651–662

Shan J, Lang D, Dimotakis P (2004) Scalar concentration measurements in liquid-phase flows with pulsed lasers. Exp Fluids 36(2):268–273

Sjöback R, Nygren J, Kubista M (1995) Absorption and fluorescence properties of fluorescein. Spectrochim Acta Part A Mol Biomol Spectrosc 51(6):L7–L21

Sutton JA, Fisher BT, Fleming JW (2008) A laser-induced fluorescence measurement for aqueous fluid flows with improved temperature sensitivity. Exp Fluids 45(5):869–881

Vetrano M, Simonini A, Steelant J, Rambaud P (2013) Thermal characterization of a flashing jet by planar laser-induced fluorescence. Exp Fluids 54(7):1573

Walker D (1987) A fluorescence technique for measurement of concentration in mixing liquids. J Phys E Sci Inst 20(2):217–224